ACS APPLIED MATERIALS & INTERFACES

Research Article

www.acsami.org

Nozzleless Fabrication of Oil-Core Biopolymeric Microcapsules by the Interfacial Gelation of Pickering Emulsion Templates

Jun-Yee Leong,[†] Beng-Ti Tey,[†,‡] Chin-Ping Tan,[§] and Eng-Seng Chan*[,†,‡]

[†]Chemical Engineering Discipline and [‡]Advanced Engineering Platform, Monash University Malaysia, Jalan Lagoon Selatan, Bandar Sunway 46150, Selangor Malaysia

[§]Department of Food Technology, Faculty of Food Science and Technology, Universiti Putra Malaysia, 43400 Serdang, Selangor Malaysia

ABSTRACT: Ionotropic gelation has been an attractive method for the fabrication of biopolymeric oil-core microcapsules due to its safe and mild processing conditions. However, the mandatory use of a nozzle system to form the microcapsules restricts the process scalability and the production of small microcapsules (<100 μm). We report, for the first time, a nozzleless and surfactant-free approach to fabricate oil-core biopolymeric microcapsules through ionotropic gelation at the interface of an O/W Pickering emulsion. This approach involves the self-assembly of calcium carbonate ($CaCO_3$) nanoparticles at the interface of O/W emulsion droplets followed by the addition of a polyanionic biopolymer into the aqueous phase. Subsequently, $CaCO_3$ nanoparticles are dissolved by pH reduction, thus liberating Ca^{2+} ions to cross-link the surrounding polyanionic biopolymer to form a shell that encapsulates the oil droplet. We demonstrate the versatility of this method by fabricating microcapsules from different types of polyanionic biopolymers (i.e., alginate, pectin, and gellan gum) and water-immiscible liquid cores (i.e., palm olein, cyclohexane, dichloromethane, and toluene). In addition, small microcapsules with a mean size smaller than 100 μm can be produced by selecting the appropriate conventional emulsification methods available to prepare the Pickering emulsion. The simplicity and versatility of this method allows biopolymeric microcapsules to be fabricated with ease by ionotropic gelation for numerous applications.

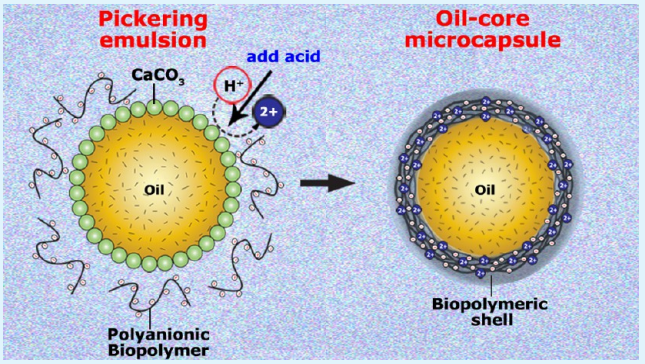

KEYWORDS: *ionotropic gelation, microcapsules, core−shell, Pickering emulsion, biopolymer*

INTRODUCTION

Microcapsules with an oil core enclosed within a polymeric shell are used in many applications for immobilization, protection, and controlled release of chemicals, fragrances, foods, or drugs.[1,2] Biopolymers derived from natural sources such as alginate, pectin, and gellan gum are gaining popularity as shell materials because they are renewable, biodegradable, and abundantly available. Because most of these biopolymers are polyanionic in nature, they can be gelled by ionotropic cross-linking with divalent cations (e.g., Ca^{2+}) at room temperature to form an insoluble matrix. This gelation method prevails over other methods in making biopolymeric microcapsules owing to its mild gelation conditions and simple process.

Among the polyanionic biopolymers, alginate is perhaps the most studied biopolymer for the fabrication of oil-core microcapsules by ionotropic gelation. In the gelation of alginate, Ca^{2+} ions form "egg-box" junction zones with alginate by ionically binding to pairs of carboxyl groups from two neighboring alginate helices.[3] This gelation mechanism has been commonly used to prepare alginate beads with the immobilized cargo dispersed throughout the polymer matrix. However, the formation of oil-core microcapsules is more challenging due to the complex capsular structure that consists of a liquid core and a solid shell. One of the approaches used to form oil-core microcapsules involves the preparation of a surfactant-stabilized W/O emulsion containing $CaCl_2$ in the aqueous phase first. The emulsion is then added dropwise into the alginate solution using a nozzle. Upon contact, the Ca^{2+} ions will cross-link the alginate polymer chains at the periphery of the emulsion droplets to form a continuous shell. The continuous outward diffusion of the Ca^{2+} across the newly formed shell results in the growth of the shell thickness. This technique has been adopted to encapsulate linalool, sunflower, and Miglyol oils in capsules of diameters ranging from 1.8 to 3.5 mm.[4,5]

In another approach, the oil phase and alginate solution can be coextruded using a two-fluid nozzle to template a compound drop consisting of an oil core and alginate shell. The alginate polymer chains will be cross-linked upon contact with the

Received: September 30, 2014
Accepted: July 6, 2015
Published: July 6, 2015

DOI: 10.1021/acsami.5b04486
ACS Appl. Mater. Interfaces 2015, 7, 16169−16176

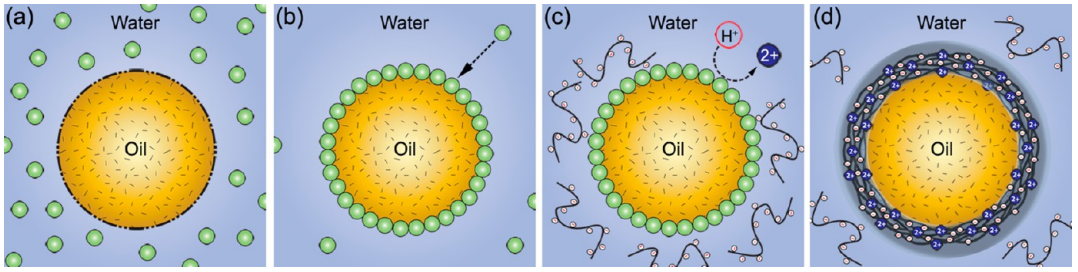

Figure 1. The process flow to fabricate a microcapsule from a Pickering emulsion template. The (a) oil phase is emulsified into an aqueous dispersion of $CaCO_3$ nanoparticles, the (b) nanoparticles adsorb at the interface to form a Pickering emulsion, then a (c) polyanionic biopolymer is introduced into the aqueous phase before the $CaCO_3$ nanoparticles are dissolved at the interface upon pH reduction to liberate Ca^{2+}, and then (d) ionotropic gelation of the liberated Ca^{2+} with the polyanionic biopolymer at the O/W interface to form a continuous shell structure.

gelation bath containing the Ca^{2+} ions. This method has been used to encapsulate phase change materials in capsules with diameters ranging from 3.5 to 4.2 mm.[6] Smaller capsules with a diameter of approximately 2 mm were fabricated using a nozzle with a smaller diameter.[7,8] The size of the capsules can also be reduced by promoting the detachment of the compound droplets from the nozzle tip by external stimuli such as vibration, electrostatic potential, or a combination of both. Oil-core capsules with a diameter as small as 0.35 to 1.61 mm were successfully produced using these methods.[9−12]

Further reduction in the capsule size can be achieved by templating a surfactant-stabilized emulsion using microfluidic devices. Ren et al. utilized a 4-nozzle microfluidic device to extrude O/W/O double emulsion droplets into a continuous stream of a $CaCl_2$ solution.[13] The Ca-alginate shell was formed when the aqueous phase in the emulsion droplet that contained the alginate polymer contacted the $CaCl_2$ solution in the continuous phase. The resultant microcapsules were approximately 0.25 mm in diameter. In another work, Liu et al. utilized a 3-nozzle microfluidic device to extrude O/W emulsion droplets into a continuous stream of an oil phase.[14] The aqueous phase of the O/W emulsion contained alginate, $CaCO_3$ particles, and a photoacid (diphenyliodonium nitrate). Downstream of the microfluidic device, the emulsion droplets were exposed to ultraviolet light to activate the photoacid and initiate the dissolution of the $CaCO_3$ particles. The released Ca^{2+} ions cross-linked the alginate in the aqueous phase internally. This method results in oil-core microcapsules approximately 0.5 mm in diameter. More recently, Duarte et al. used a 3-nozzle microfluidic device to disperse oil-core alginate-shell compound droplets with a coaxial air flow.[15] The compound droplets were collected in a $CaCl_2$ solution to harden the shell. Perfluorocarbon was successfully encapsulated in microcapsules with diameters between 0.11 and 0.13 mm.

From the literature, it is obvious that the formation of oil-core capsules using ionotropic gelation involves the mandatory use of a nozzle, and this requirement results in two inevitable problems. First, the size of the microcapsules is limited by the nozzle diameter. Although the size of the capsule can be reduced by using a smaller nozzle, reducing the nozzle diameter gives rise to a larger pressure drop during the production, as well as increases the tendency of a nozzle blockage. Miniaturization of nozzles using microfluidic devices is also complicated, with difficulties experienced in controlling the fluid flow and droplet breakup from multiple liquid streams. Second, using the nozzle approach, the microcapsules are produced in a drop-by-drop manner. This seriously limits the productivity of the process, especially when small microcapsules are desired. The only way to increase the productivity is through the parallelization of nozzles. However, this approach is economically and technically challenging. These two limitations may impose a bottleneck for producing oil-core biopolymeric microcapsules via ionotropic gelation for a variety of applications. A very recent work by Martins et al. showed that it was possible to produce oil-core microcapsules without the use of a nozzle by pouring an O/W/O double emulsion containing $CaCl_2$ in the water phase into an alginate solution.[16] However, this method requires complex formulation of the emulsions as well as careful control over the processing conditions (e.g., pouring rate of emulsions or stirring rate of alginate solution) in order to form oil-core microcapsules.

Pickering emulsions are emulsions stabilized by solid particles that are adsorbed at the O/W interface.[17] Solid particles larger than a few nanometers adsorb virtually irreversibly at the O/W interface and act as a physical barrier for material transfer.[18] The Pickering emulsion has exceptional stability against coalescence and can be prepared easily using conventional emulsification methods. The "surfactant-free" character makes them attractive in several fields where surfactants often show adverse effects such as irritancy and hemolytic behavior.[19] In recent years, significant efforts have been geared toward the use of Pickering emulsions as a template to make advanced materials for applications in imaging, encapsulation, and controlled drug release.[20] The solid particles adsorbed at the O/W interface can be bridged and transformed into a continuous shell through various methods, which include sintering with heat, covalent cross-linking, inducing van der Waals forces, spontaneous jamming, and the adsorption of polymer.[21−25] Examples of the solid particles that have been used to form Pickering emulsions include polystyrene, silica, TiO_2, $CaCO_3$, etc.[26−29]

In this work, we combine the concepts of ionotropic gelation and Pickering emulsion by performing ionic cross-linking of polyanionic biopolymers at the interface of an O/W emulsion stabilized by $CaCO_3$ nanoparticles. Our fabrication process consists of four steps as illustrated in Figure 1. First, an oil phase is emulsified into a dispersion of $CaCO_3$ nanoparticles. Second, the $CaCO_3$ nanoparticles are allowed to self-assemble at the O/W interface. Third, a polyanionic biopolymer is introduced into the aqueous phase of the Pickering emulsion. The pH of the emulsion is subsequently reduced to dissolve the $CaCO_3$ nanoparticles. Finally, the Ca^{2+} ions are liberated upon the dissolution of the $CaCO_3$, which cross-links the polyanionic biopolymer at the periphery to form a continuous shell that envelops the oil core. This results in the formation of biopolymeric oil-core microcapsules. The versatility of this

DOI: 10.1021/acsami.5b04486
ACS Appl. Mater. Interfaces 2015, 7, 16169−16176

Table 1. Experimental Conditions To Prepare O/W Pickering Emulsion Templates Stabilized by $CaCO_3$ Nanoparticles

	experimental conditions				
emulsification method	rotation speed (rpm)	pressure (kPa)	duration (min)	volume of oil (mL)	volume of $CaCO_3$ dispersion (mL)
mechanical stirrer	600		30	150	350
high speed homogenizer	5000		30	150	350
SPG membrane (500 nm pore size)	500	210	30	60	140

method is demonstrated by fabricating the microcapsules using different polyanionic biopolymers, water-immiscible liquids, and emulsification methods.

EXPERIMENTAL SECTION

Chemicals and Materials. Sodium alginate (Manugel GHB) was purchased from FMC Biopolymers, U.K. Gellan gum (KELCOGEL) and pectin (GENU, LM-14 AG) were purchased from CP Kelco, Denmark. Refined, bleached, and deodorized (RBD) palm olein was purchased from Lam Soon Edible Oils (M) Sdn Bhd, Malaysia. Cyclohexane, dichloromethane, toluene, and $CaCl_2$ dehydrate (AR grade) were purchased from Fisher Scientific, U.K. Glacial acetic acid (AR grade) was purchased from Fluka Chemika, Switzerland. The $CaCO_3$ nanoparticles (NPCC-111) were a generous gift from NanoMaterials Technology Pte. Ltd., Singapore. All chemicals were used as received.

Characterization of $CaCO_3$ Nanoparticles. The $CaCO_3$ nanoparticles were dispersed in ultrapure water using a high shear homogenizer (Microfluidics model M-110P Microfluidizer) operated with Z-flow cell at 22 000 psi for 4 passes to yield a concentration of 50 mg mL^{-1}. A drop of the suspension was air-dried at room temperature. The dried sample was then sputter-coated with gold for observation by field emission scanning electron microscopy (Hitachi model S3400N-II, Japan). The size analysis was performed on a dilute dispersion of $CaCO_3$ using a Zetasizer (Malvern model Nano ZS, U.K.).

Preparation of O/W Pickering Emulsion. Palm olein was emulsified into the $CaCO_3$ dispersion (5% w/v) using three different types of emulsification tools: a mechanical stirrer (IKA model EUROSTAR power control-visc P1, Gemany), a high speed homogenizer (IKA model Ultra-Turrax T-25, Germany), and a Shirasu porous glass (SPG) membrane (SPG Technology model MG-20, Japan). For the other water-immiscible liquids investigated (cyclohexane, dichloromethane, and toluene), the O/W Pickering emulsions were prepared by a high speed homogenizer. The emulsification conditions are described in Table 1. The resultant Pickering emulsion was allowed to phase separate for 24 h prior to use and further characterization.

Fabrication of Oil-Core Microcapsules. The creamy layer (5 mL) of the phase-separated O/W Pickering emulsion was redispersed into 100 mL of a polyanionic biopolymer solution of an appropriate concentration (2.5% w/v sodium alginate, 2.0% w/v gellan gum, or 2.0% w/v pectin) under gentle stirring for 15 min. Acetic acid at a concentration of 1 M was added drop-by-drop into the Pickering emulsion until the pH reached 4 to dissolve the $CaCO_3$ nanoparticles and to initiate the ionotropic gelation at the periphery of the oil droplets. The pH of the dispersion was monitored and maintained throughout the gelation process. The ionotropic gelation process was allowed to continue for 60 min before the dispersion was diluted with 2 L of ultrapure water. The microcapsules that formed were decanted and stored in ultrapure water for further characterization.

Preparation of Biopolymer Films. Dried calcium-cross-linked films for each biopolymer were fabricated as controls, and their surface morphologies were compared with that of the microcapsules formed. In brief, 50 mL of 2% w/v $CaCl_2$ solution was injected slowly into a Petri dish containing 10 mL of biopolymer solution of an appropriate concentration (2.5% w/v sodium alginate, 2.0% w/v gellan gum, or 2.0% w/v pectin). Upon contact with $CaCl_2$ solution, the biopolymer solution gelled instantaneously. The formed hydrogel slab was left immersed in the $CaCl_2$ solution for 30 min for curing. The hydrogel slab was rinsed with ultrapure water and oven-dried into a film at 80 °C for 24 h.

Interfacial Adsorption Measurements. The dynamic interfacial tension between the oil and aqueous phase in the presence of $CaCO_3$ nanoparticles at the interface was studied using the inverted drop method conducted on a goniometer (ramé-hart model 100). The built-in software acquired the image of a drop over time and fit the shape profile with the Young Laplace equation in order to obtain the corresponding interfacial tension. A 2 μL portion of the oil phase was extruded from a U-shaped syringe needle using a microsyringe to form an inverted pendant drop that hung on the needle tip. The extrusion was conducted in a dispersion of $CaCO_3$ nanoparticles with concentration up to 0.01% w/v. Drop shape imaging was not possible at $CaCO_3$ concentration higher than 0.01% w/v due to strong interference in the background.

Characterization of O/W Pickering Emulsions, Microcapsules, and Biopolymer Films. The sizes of the Pickering emulsion droplets and microcapsules were measured using a Mastersizer (Malvern model 3000 Hydro, U.K.). Optical microscopy images of the O/W Pickering emulsions and microcapsules were taken with an inverted optical microscope (Nikon model Eclipse TS100, Japan). Confocal laser scanning microscopy (CLSM) images of the microcapsules were acquired using a laser scanning microscope (Leica model TCS SP2, Germany) with Fluo-3 as the fluorescent markers for Ca^{2+}. Macroscopic view of the microcapsules was visualized using a scanning electron microscope (SEM) (Hitachi model S-3400, Japan) operated at an accelerating voltage of 10 kV. The microcapsules were oven-dried at 80 °C for 24 h prior to the SEM analysis. Fourier transform infrared (FT-IR) spectra of the raw materials (i.e., biopolymer powder, palm olein, and $CaCO_3$ nanoparticles) and oven-dried microcapsules were obtained from an FT-IR spectrometer (Nicolet model iS10). The FT-IR spectrometer was operated at an average of 64 scans from 650 to 4000 cm^{-1} with a resolution of 4 cm^{-1} at 25 °C. The FT-IR spectra of the microcapsules and the respective powder for each biopolymer were offset to the same baseline (i.e., at 100% transmittance) for better readability. FESEM images of surface profiles of the microcapsules and biopolymer films were captured using a Hitachi S3400N-II field emission scanning electron microscope operated at an accelerating voltage 1−2 kV. The dried microcapsules and the biopolymer films were sputter-coated with Au prior to FESEM analysis.

RESULTS AND DISCUSSION

In the present study, $CaCO_3$ nanoparticles were used for two main reasons: to stabilize the O/W emulsions, and to provide a source of Ca^{2+} ions for cross-linking with alginate at the O/W interface. $CaCO_3$ is also inexpensive and nontoxic. The $CaCO_3$ nanoparticles were suspended in ultrapure water and dispersed using a high shear homogenizer. The $CaCO_3$ nanoparticles are cubical, and no aggregates are observed by FESEM (see Figure 2a). The size distribution of the $CaCO_3$ nanoparticles is monomodal, ranging between 100 and 400 nm (see Figure 2b). The mean size is approximately 200 nm.

The self-assembly of the colloidal particles at the liquid−liquid interface is governed by the Stoke−Einstein relationship if there are no attractive forces driving the particles toward the interface.[30] The adsorption process is favored if the interfacial energy between the two fluids exceeds the difference in surface energies between the colloids and the internal fluid, and

DOI: 10.1021/acsami.5b04486
ACS Appl. Mater. Interfaces 2015, 7, 16169−16176

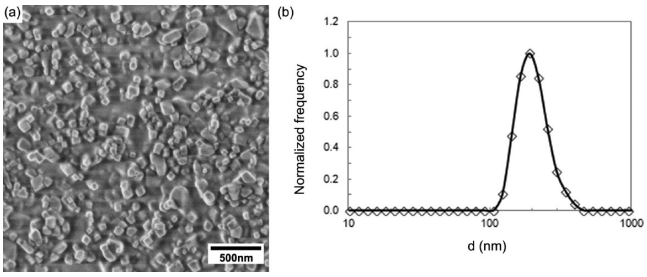

Figure 2. The $CaCO_3$ nanoparticles used in the preparation of Pickering emulsion templates for microcapsules fabrication were in cubical shapes with no aggregates as shown in (a) FESEM image, and the (b) particle size distribution was unimodal. Scale bar in part a is 500 nm.

between the colloids and the external fluid.[31] In order to verify the adsorption of $CaCO_3$ at the O/W interface, an indirect measurement method was adopted to investigate the changes in interfacial energy of the immiscible liquids upon the addition of nanoparticles. Upon adsorption of a solid at an interface, a portion of the liquid–liquid interface will be replaced by the solid and lead to the reduction in the total interfacial energy.

The reduction of the dynamic interfacial tension between the palm olein and pure water due to the adsorption of $CaCO_3$ nanoparticles at the O/W interface is plotted in Figure 3. The

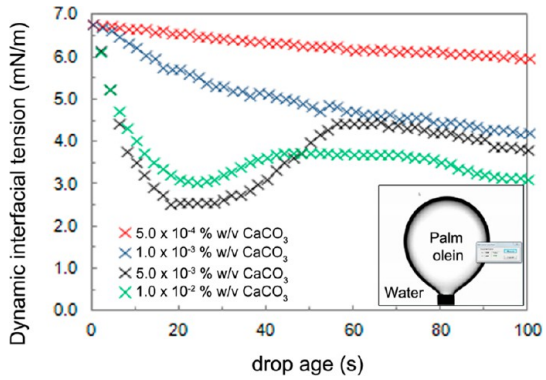

Figure 3. The dynamic interfacial tension of palm olein and pure water during the adsorption of $CaCO_3$ nanoparticles at different $CaCO_3$ concentrations. Reduction in the dynamic interfacial tension over time indicates the adsorption of $CaCO_3$ at the O/W interface. The inset shows the inverted pendant drop of palm olein during the adsorption of $CaCO_3$ at the O/W interface.

dynamic interfacial tension of the immiscible liquids reduced more rapidly and in greater amplitude at higher $CaCO_3$ concentrations. Even within a short time frame of 100 s, a clear difference in the reduction profiles of the interfacial energy was observed for different $CaCO_3$ concentrations. At the lowest $CaCO_3$ concentration, the dynamic interfacial tension did not deviate significantly from the initial value of 6.8 mN/m. On the other hand, the initial interfacial tension dropped by approximately 50% within 100 s at the highest $CaCO_3$ concentration. This observation was expected because the initial coverage or adsorption of $CaCO_3$ at the interface was diffusion dominated. Therefore, a higher initial concentration led to a greater flux of $CaCO_3$ nanoparticles toward the O/W interface. The reduction in the interfacial tension indicates that the $CaCO_3$ nanoparticles were adsorbed onto the O/W interface.

We will first describe the formation of microcapsules using alginate as the model polyanionic biopolymer. Figure 4 shows the CLSM of a microcapsule prepared using membrane emulsification. The microcapsules formed using this method were between 1 and 110 μm in diameter (see Figure 5c). The microcapsules were labeled with Fluo-3, a fluorescent Ca^{2+} indicator that can be excited at 450 nm upon binding with Ca^{2+}. A small microcapsule (<5 μm) was selected for the ease of performing the z-stack imaging using a confocal microscope. The images reveal the core–shell structure of the microcapsule with Ca^{2+} (fluorescence) covering the periphery of the microcapsule (see Figure 4a). The Ca^{2+} ions cross-linked the alginate polymer chains to form the shell structure of the microcapsule. The thickness of the shell was approximately 1 μm, enveloping a core of approximately 2 μm in diameter (see Figure 4b).

Figure 5 depicts the size distribution of the palm olein-water Pickering emulsions and their resultant oil-core Ca-alginate microcapsules fabricated using different emulsification methods, i.e., mechanical stirrer, high speed homogenizer, and SPG membrane. Microcapsules prepared using a mechanical stirrer showed the largest size with diameters ranging from 60 to 400 μm with a mean value of approximately 200 μm. The size distribution of the microcapsules was unimodal with a span value of 0.96. On the other hand, the microcapsules prepared using a high speed homogenizer had a size ranging from 10 to 280 μm with a mean value of 43 μm. The size distribution of the microcapsules was bimodal with a span value of 1.26. The microcapsules prepared using a SPG membrane had the smallest size with diameters ranging from 1 to 110 μm with a mean value of 42 μm. The size distribution was bimodal with a span value of 1.37. These results demonstrate that microcapsules can be produced using different emulsification methods and that the size of the microcapsules can be easily tuned by selecting the appropriate method. In addition, the results also show that the microcapsules formed were slightly larger compared their corresponding emulsion droplets. This observation was expected because the Ca-alginate shell thickness contributed to the size of the microcapsules.

The versatility of the method was tested by fabricating the microcapsules from two other polyanionic biopolymers, i.e., gellan gum and pectin. Gellan gum and pectin are natural polysaccharides that are extracted from microbial fermentation and plant cell walls, respectively. Similar to alginate, these two polyanionic biopolymers are able to form gels upon ionic cross-linking with Ca^{2+}. The microcapsules prepared were analyzed using FT-IR spectroscopy. Figure 6 shows the FT-IR bands of the microcapsules made from Ca-alginate, Ca-gellan gum, and Ca-pectinate. The FT-IR spectra of the sodium alginate showed peaks at 3426, 1595, 1405, and 1032 cm^{-1} that correspond to the stretching of O–H, COO^- (asymmetric), COO^- (symmetric), and C–O–C bonds, respectively.

For the Ca-alginate microcapsules, the O–H stretching was narrower and had a greater intensity, indicating an increase in the intramolecular bonding between the biopolymer strands. The asymmetric COO^- stretching was broader, indicating that there is a stronger interaction between the asymmetric COO^- groups and Ca^{2+} ions. The symmetric COO^- stretching shifted to a higher wavenumber of 1416 cm^{-1}, a peak that is specific to ionic bonding. The charge density, radius, and atomic weight of Ca^{2+} changed during the ion exchange with Na^+ in the alginate, thus creating a new environment around the carbonyl groups of alginate. Furthermore, the band that corresponds to the C–O–

DOI: 10.1021/acsami.5b04486
ACS Appl. Mater. Interfaces 2015, 7, 16169–16176

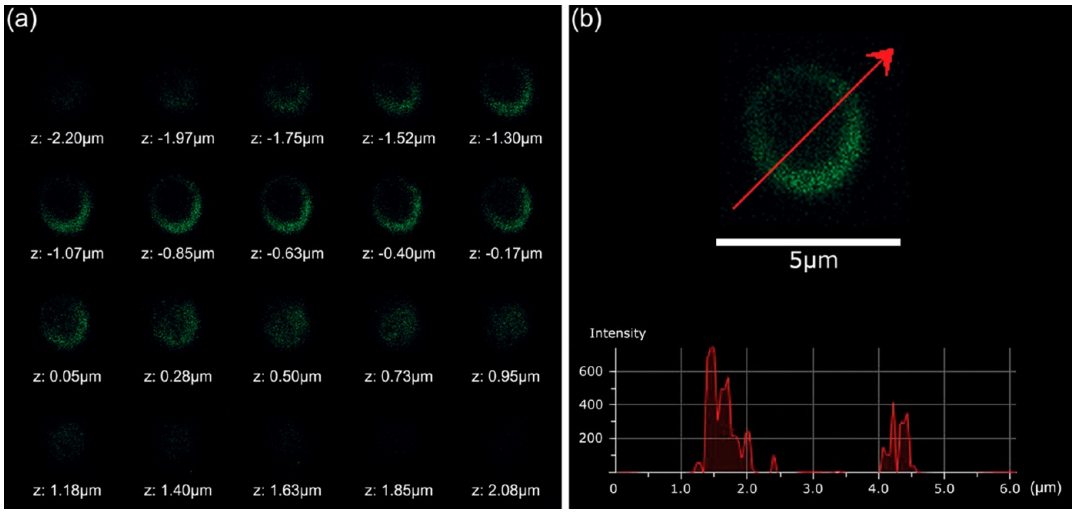

Figure 4. Ca-alginate microcapsule fabricated from a Pickering emulsion template using the SPG membrane: (a) z-sectioning and (b) cross-sectional CLSM image reveal a core-shell structure of the microcapsule labeled with Fluo-3.

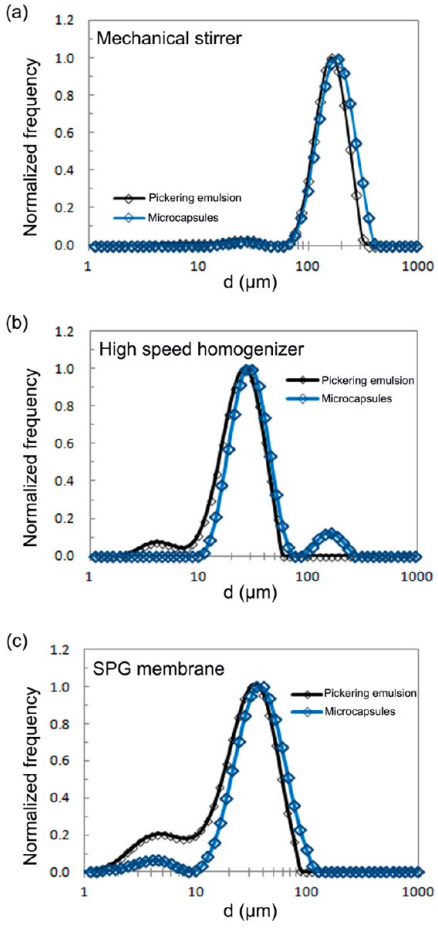

Figure 5. Size distribution of the palm olein-water Pickering emulsions and their corresponding microcapsules fabricated using a (a) mechanical stirrer, (b) high speed homogenizer, and (c) SPG membrane. The results indicate that microcapsule size can be varied by selecting different emulsification methods.

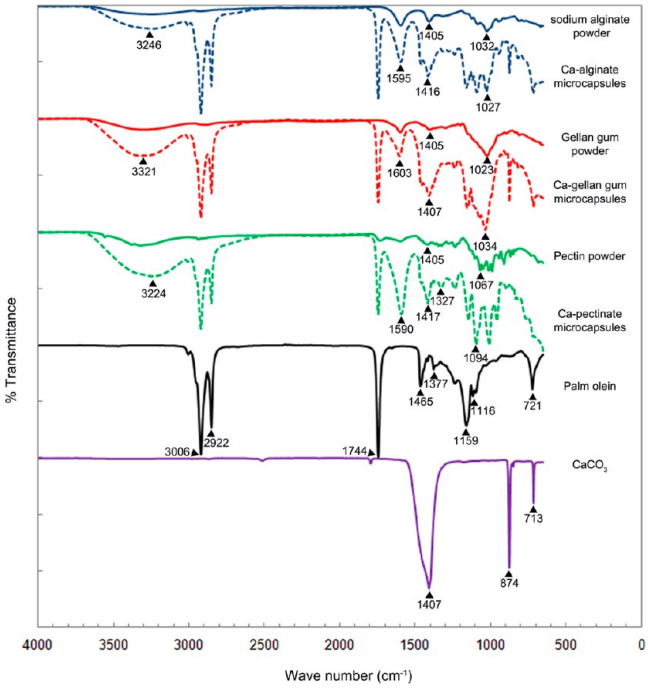

Figure 6. FT-IR spectra of the ionotropically cross-linked microcapsules fabricated using alginate, gellan gum, and pectin, as compared to the pristine samples of biopolymers in powder form. Spectra have been offset for better readability. Units of the *y*-axis are arbitrary. FT-IR spectra show the presence of palm olein and residue $CaCO_3$ in the microcapsules.

C stretching shifted to a lower wavenumber of 1027 cm^{-1}, indicating weakened bonding as the bonds are now being shared with Ca^{2+} ions. All these observations are typical changes observed in the FT-IR spectra of alginate upon ionic cross-linking with Ca^{2+}.[32] Similar changes were observed for FT-IR spectra of the Ca-gellan gum and the Ca-pectinate microcapsules, thus confirming the ionic cross-linking of the polyanionic biopolymers with Ca^{2+}.[33,34]

The FT-IR spectra of the microcapsules indicate the presence of palm olein and $CaCO_3$. The presence of palm olein was detected at 3006, 2922, and 1159 cm^{-1} because the microcapsules were broken when being pinned to the sample holder when performing the FT-IR analysis, thus exposing the core (palm olein). On the other hand, the peaks attributed to the $CaCO_3$ were detected at 874 cm^{-1}, indicating the presence

DOI: 10.1021/acsami.5b04486
ACS Appl. Mater. Interfaces 2015, 7, 16169−16176

of residual $CaCO_3$ in the microcapsules due to the incomplete dissolution of the $CaCO_3$ during microcapsule formation.

The surface morphologies of the dried oil-core microcapsules made of Ca-alginate, Ca-gellan gum, and Ca-pectinate were examined using FESEM (Figure 7a–c). Dried calcium-cross-linked films for each biopolymer were also fabricated as controls, and their surface morphologies are compared with that of the microcapsules formed (Figure 7d–f). The surface morphologies of the microcapsules and films for each biopolymer were found to be identical with the same pattern of wrinkles, thus verifying the formation of calcium-cross-linked biopolymer shells on the microcapsules. Wrinkles were formed on the surface of the microcapsules and films as a result of the shrinkage of hydrogel matrices during drying.

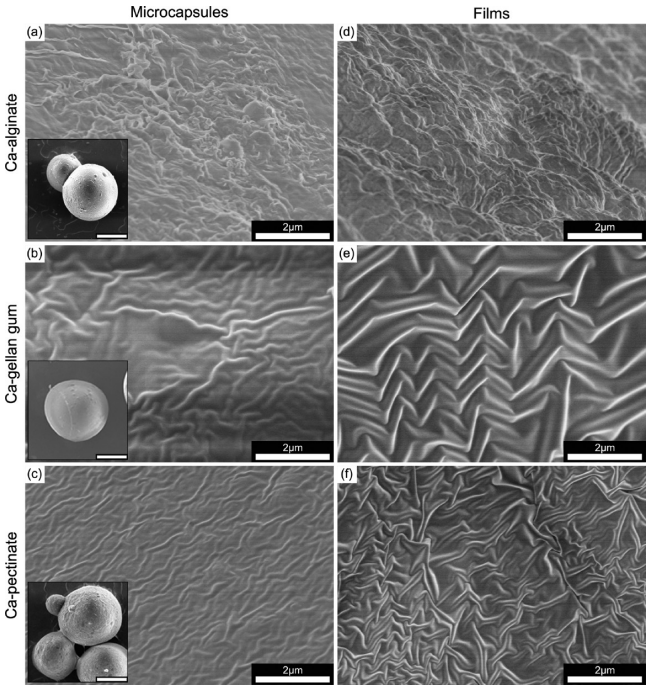

Figure 7. Surface morphology of the dried microcapsules (a–c) is analogous to the dried biopolymer films (d–f) fabricated from Ca-alginate, Ca-gellan gum, and Ca-pectinate. The insets show the macroscopic views of microcapsules prepared using mechanical stirrer. Scale bars in insets represent 200 μm.

However, the surfaces of the microcapsules were found to contain fewer wrinkles than the films. This finding is likely caused by the lower concentration of polymer on the surface of the microcapsules compared to the films. During the formation of the microcapsules, the $CaCO_3$ at the O/W interface solubilized to liberate the Ca^{2+} ions to cross-link the adjacent biopolymer chains instantly to form a thin shell. The excess Ca^{2+} ions would diffuse outward through the shell to cross-link with the free biopolymer chains in the bulk solution that consequently thickened the shell in an outward direction. As the process continued, the concentration of Ca^{2+} ions available for cross-linking would decrease, resulting in a lower degree of cross-linking at the surface of the shell compared to that of the innermost layer of the shell. This means that a looser polymer network would have formed at the surface of the microcapsules, allowing more room for reorganization during the drying process and thus resulting in fewer surface wrinkles.

On the contrary, the biopolymer films were formed by the biopolymer solutions coming in contact with excess Ca^{2+} ions. Under these conditions, the cross-linking density of the whole hydrogel slab formed would be uniform, thus forming a compact polymer network even at the surface of the hydrogel slab. This compact polymer network would have less space for reorganization during drying, thus resulting in more wrinkles formed compared to those of the microcapsules.

The feasibility of this method to encapsulate a water-immiscible liquid with different characteristics was also evaluated. Palm olein, cyclohexane, dichloromethane, and toluene were used because they have different viscosities, dielectric constants, and polarities (see Table 2). O/W

Table 2. Characteristics of Different Water-Immiscible Liquids[a]

property	palm olein	cyclohexane	dichloromethane	toluene
absolute viscosity (25 °C, cP)	41.9	0.98	0.44	0.59
dielectric constant (20 °C)	3.2	2.01	29.1	2.38
relative polarity (water = 100)	n.a.[b]	0.6	30.9	9.9

[a]Data extracted from Smallwood.[35] [b]n.a. data not available.

Pickering emulsions stabilized by $CaCO_3$ nanoparticles were successfully prepared with all types of water-immiscible liquids investigated (Figure 8a–d) using a high speed homogenizer. The O/W Pickering emulsions formed were found to be stable against coalescence. The partial wettability of $CaCO_3$ by most common oils,[19] and therefore the strong anchoring force at the O/W interface, might contribute to the stability of the emulsions. All the oil droplets in the Pickering emulsions appeared to have rough surface due to the presence of $CaCO_3$ nanoparticles at the O/W interface.

Subsequently, microcapsules were successfully fabricated from these emulsions (Figure 8e–h) using alginate as the model polyanionic biopolymer. In comparison to the Pickering emulsion, the surface of the microcapsules formed was clean and smooth regardless of the type of liquid-core used, indicating the successful formation of a hydrogel shell. The results suggest that this method can be used to encapsulate a wide range of water-immiscible liquids including solvents, thus revealing its potential for application in diverse fields including pharmaceuticals, food, inks, paints, detergents, pesticides, textiles, etc.

CONCLUSION

A novel nozzleless and surfactant-free method to fabricate oil-core biopolymeric microcapsules through ionotropic gelation at the O/W interface of a Pickering emulsion has been developed. The method can be easily performed under ambient conditions using conventional emulsification methods, without the use of surfactant. Microcapsules have been successfully fabricated using three different types of polyanionic biopolymers (i.e., alginate, gellan gum, and pectin). We also show the versatility of this method by successfully encapsulating a variety of water-immiscible liquids with different properties (viscosity, polarity, and dielectric constant), including solvents such as cyclohexane, dichloromethane, and toluene. The mean size of the microcapsules ranged between 40 and 200 μm, and the size can be tuned using the appropriate emulsification method. The

DOI: 10.1021/acsami.5b04486
ACS Appl. Mater. Interfaces 2015, 7, 16169–16176

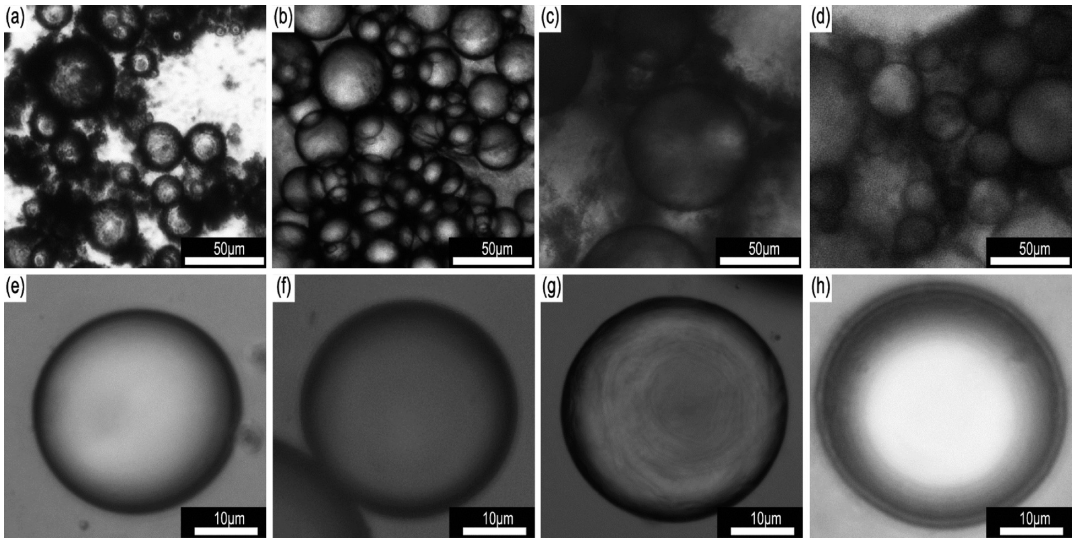

Figure 8. Optical images of the (a) palm olein, (b) cyclohexane, (c) dichloromethane, and (d) toluene O/W Pickering emulsions stabilized by $CaCO_3$ nanoparticles showing rough surfaces due to the presence of $CaCO_3$ nanoparticles. Their resulting microcapsules in parts e, f, g, and h, respectively, show smoother surfaces.

simplicity and versatility of this method allows for the production of microcapsules in various fields for controlled-release or chemical-on-demand applications.

AUTHOR INFORMATION

Corresponding Author

*E-mail: chan.eng.seng@monash.edu.

Author Contributions

This manuscript was written with contributions from all authors. All authors have given approval to the final version of this manuscript.

Notes

The authors declare no competing financial interest.

ACKNOWLEDGMENTS

The authors thank the Ministry of Science, Technology and Innovation (MOSTI) for the financial support for this work (eScience project number: 06-02-10-SF0157) and the School of Engineering, Monash University Malaysia, for providing the Ph.D. studentship for Jun-Yee Leong.

REFERENCES

(1) McClements, D. J.; Decker, E. A.; Park, Y.; Weiss, J. Designing Food Structure to Control Stability, Digestion, Release and Absorption of Lipophilic Food Components. *Food Biophys.* **2008**, *3*, 219−228.

(2) Matalanis, A.; Jones, O. G.; McClements, D. J. Structured Biopolymer-based Delivery Systems for Encapsulation, Protection, and Release of Lipophilic Compounds. *Food Hydrocolloids* **2011**, *25*, 1865−1880.

(3) Grant, G. T.; Morris, E. R.; Rees, D. A.; Smith, P. J.; Thom, D. Biological Interactions between Polysaccharides and Divalent Cations: The Egg-box Model. *FEBS Lett.* **1973**, *32*, 195−198.

(4) Abang, S.; Chan, E. S.; Poncelet, D. Effects of Process Variables on the Encapsulation of Oil in Ca-alginate Capsules Using An Inverse Gelation Technique. *J. Microencapsulation* **2012**, *29*, 417−428.

(5) Lopez, M. D.; Maudhuit, A.; Pascual-Villalobos, M. J.; Poncelet, D. Development of Formulations to Improve the Controlled-release of Linalool to be Applied as an Insecticide. *J. Agric. Food Chem.* **2012**, *60*, 1187−1192.

(6) Liang, W. G.; Yang, C.; Wen, G. Q.; Wang, W.; Ju, X. J.; Xie, R.; Chu, L. Y. A Facile and Controllable Method to Encapsulate Phase Change Materials with Non-toxic and Biocompatible Chemicals. *Appl. Therm. Eng.* **2014**, *70*, 817−826.

(7) Kurayama, F.; Yoshikawa, T.; Furusawa, T.; Bahadur, N. M.; Handa, H.; Sato, M.; Suzuki, N. Microcapsule with a Heterogeneous Catalyst for The Methanolysis of Rapeseed Oil. *Bioresour. Technol.* **2013**, *135*, 652−658.

(8) Bremond, N.; Santanach-Carreras, E.; Chu, L. Y.; Bibette, J. Formation of Liquid-core Capsules Having a Thin Hydrogel Membrane: Liquid Pearls. *Soft Matter* **2010**, *6*, 2484−2488.

(9) Phawaphuthanon, N.; Behnam, S.; Koo, S. Y.; Pan, C. H.; Chung, D. Characterization of Core−shell Calcium-alginate Macrocapsules Fabricated by Electro-coextrusion. *Int. J. Biol. Macromol.* **2014**, *65*, 267−274.

(10) Wang, W.; Waterhouse, G. I.; Sun-Waterhouse, D. Co-extrusion Encapsulation of Canola Oil with Alginate: Effect of Quercetin Addition to Oil Core and Pectin Addition to Alginate Shell on Oil Stability. *Food Res. Int.* **2013**, *54*, 837−851.

(11) Whelehan, M.; von Stockar, U.; Marison, I. W. Removal of Pharmaceuticals from Water: Using Liquid-core Microcapsules as a Novel Approach. *Water Res.* **2010**, *44*, 2314−2324.

(12) Wyss, A.; Boucher, J.; Montero, A.; Marison, I. Micro-encapsulated Organic Phase for Enhanced Bioremediation of Hydrophobic Organic Pollutants. *Enzyme Microb. Technol.* **2006**, *40*, 25−31.

(13) Ren, P. W.; Ju, X. J.; Xie, R.; Chu, L. Y. Monodisperse Alginate Microcapsules with Oil Core Generated from a Microfluidic Device. *J. Colloid Interface Sci.* **2010**, *343*, 392−395.

(14) Liu, L.; Wu, F.; Ju, X. J.; Xie, R.; Wang, W.; Niu, C. H.; Chu, L. Y. Preparation of Monodisperse Calcium Alginate Microcapsules via Internal Gelation in Microfluidic-generated Double Emulsions. *J. Colloid Interface Sci.* **2013**, *404*, 85−90.

(15) Duarte, A. R. C.; Ünal, B.; Mano, J. F.; Reis, R. L.; Jensen, K. F. Microfluidic Production of Perfluorocarbon-Alginate Core−Shell Microparticles for Ultrasound Therapeutic Applications. *Langmuir* **2014**, *30*, 12391−12399.

(16) Martins, E.; Renard, D.; Davy, J.; Marquis, M.; Poncelet, D. Oil Core Microcapsules by Inverse Gelation Technique. *J. Micro-encapsulation* **2015**, *32*, 86−95.

(17) Pickering, S. U. CXCVI.—Emulsions. *J. Chem. Soc., Trans.* **1907**, *91*, 2001−2021.

(18) Du, K.; Glogowski, E.; Emrick, T.; Russell, T. P.; Dinsmore, A. D. Adsorption Energy of Nano-and Microparticles at Liquid− liquid Interfaces. *Langmuir* **2010**, *26*, 12518−12522.

DOI: 10.1021/acsami.5b04486
ACS Appl. Mater. Interfaces 2015, 7, 16169−16176

(19) Chevalier, Y.; Bolzinger, M. A. Emulsions Stabilized with Solid Nanoparticles: Pickering Emulsions. *Colloids Surf., A* **2013**, *439*, 23−34.
(20) Rossier-Miranda, F. J.; Schroën, C. G. P. H.; Boom, R. M. Colloidosomes: Versatile Microcapsules in Perspective. *Colloids Surf., A* **2009**, *343*, 43−49.
(21) Hsu, M. F.; Nikolaides, M. G.; Dinsmore, A. D.; Bausch, A. R.; Gordon, V. D.; Chen, X.; Hutchinson, J. W.; Weitz, D. A.; Marquez, M. Self-assembled Shells Composed of Colloidal Particles: Fabrication and Characterization. *Langmuir* **2005**, *21*, 2963−2970.
(22) Croll, L. M.; Stöver, H. D. Mechanism of Self-assembly and Rupture of Cross-linked Microspheres and Microgels at the Oil-water Interface. *Langmuir* **2003**, *19*, 10077−10080.
(23) Noble, P. F.; Cayre, O. J.; Alargova, R. G.; Velev, O. D.; Paunov, V. N. Fabrication of "Hairy" Colloidosomes with Shells of Polymeric Microrods. *J. Am. Chem. Soc.* **2004**, *126*, 8092−8093.
(24) Subramaniam, A. B.; Abkarian, M.; Stone, H. A. Controlled Assembly of Jammed Colloidal Shells on Fluid Droplets. *Nat. Mater.* **2005**, *4*, 553−556.
(25) Dinsmore, A. D.; Hsu, M. F.; Nikolaides, M. G.; Marquez, M.; Bausch, A. R.; Weitz, D. A. Colloidosomes: Selectively Permeable Capsules Composed of Colloidal Particles. *Science* **2002**, *298*, 1006−1009.
(26) Binks, B. P.; Lumsdon, S. O. Pickering Emulsions Stabilized by Monodisperse Latex Particles: Effects of Particle Size. *Langmuir* **2001**, *17*, 4540−4547.
(27) Frelichowska, J.; Bolzinger, M. A.; Chevalier, Y. Pickering Emulsions with Bare Silica. *Colloids Surf., A* **2009**, *343*, 70−74.
(28) Chen, T.; Colver, P. J.; Bon, S. A. Organic−Inorganic Hybrid Hollow Spheres Prepared from TiO_2-Stabilized Pickering Emulsion Polymerization. *Adv. Mater.* **2007**, *19*, 2286−2289.
(29) Zhu, Y.; Lu, L. H.; Gao, J.; Cui, Z. G.; Binks, B. P. Effect of Trace Impurities in Triglyceride Oils on Phase Inversion of Pickering Emulsions Stabilized by $CaCO_3$ Nanoparticles. *Colloids Surf., A* **2013**, *417*, 126−132.
(30) Kutuzov, S.; He, J.; Tangirala, R.; Emrick, T.; Russell, T. P.; Böker, A. On the Kinetics of Nanoparticle Self-assembly at Liquid/liquid Interfaces. *Phys. Chem. Chem. Phys.* **2007**, *9*, 6351−6358.
(31) Kralchevsky, P. A.; Nagayama, K. Capillary Interactions between Particles Bound to Interfaces, Liquid Films and Biomembranes. *Adv. Colloid Interface Sci.* **2000**, *85*, 145−192.
(32) Sartori, C.; Finch, D. S.; Ralph, B.; Gilding, K. Determination of the Cation Content of Alginate Thin Films by FTi. r. Spectroscopy. *Polymer* **1997**, *38*, 43−51.
(33) Yang, F.; Xia, S.; Tan, C.; Zhang, X. Preparation and Evaluation of Chitosan-Calcium-Gellan Gum Beads for Controlled Release of Protein. *Eur. Food Res. Technol.* **2013**, *237*, 467−479.
(34) Wellner, N.; Kačuráková, M.; Malovíková, A.; Wilson, R. H.; Belton, P. S. FT-IR Study of Pectate and Pectinate Gels Formed by Divalent Cations. *Carbohydr. Res.* **1998**, *308*, 123−131.
(35) Smallwood, I. M. *Handbook of Organic Solvent Properties*; Elsevier: Amsterdam, 1996.

DOI: 10.1021/acsami.5b04486
ACS Appl. Mater. Interfaces 2015, 7, 16169−16176